The EMBO Journal vol.15 no.7 pp.1572–1582, 1996

Proteolytic cleavage of the urokinase receptor substitutes for the agonist-induced chemotactic effect

Massimo Resnati[1,2], Maria Guttinger[1], Simona Valcamonica[1,2], Nicolai Sidenius[1,2], Francesco Blasi[1,2] and Francesca Fazioli[1,2,3]

[1]Department of Biology and Biotechnology, San Raffaele Scientific Institute, Via Olgettina 60, 20132 Milano and [2]Department of Genetics and Microbial Biology, University of Milan, Milano, Italy

[3]Corresponding author

Physiological concentrations of urokinase plasminogen activator (uPA) stimulated a chemotactic response in human monocytic THP-1 through binding to the urokinase receptor (uPAR). The effect did not require the protease moiety of uPA, as stimulation was achieved also with the N-terminal fragment (ATF), while the 33 kDa low molecular weight uPA was ineffective. Co-immunoprecipitation experiments showed association of uPAR with intracellular kinase(s), as demostrated by *in vitro* kinase assays. Use of specific antibodies identified p56/p59^{hck} as a kinase associated with uPAR in THP-1 cell extracts. Upon addition of ATF, p56/p59^{hck} activity was stimulated within 2 min and returned to normal after 30 min. Since uPAR lacks an intracellular domain capable of interacting with intracellular kinases, activation of p56/p59^{hck} must require a transmembrane adaptor. Evidence for this was strongly supported by the finding that a soluble form of uPAR (suPAR) was capable of inducing chemotaxis not only in THP-1 cells but also in cells lacking endogenous uPAR (IC_{50}, 5 pM). However, activity of suPAR required chymotrypsin cleavage between the N-terminal domain D1 and D2 + D3. Chymotrypsin-cleaved suPAR also induced activation of p56/p59^{hck} in THP-1 cells, with a time course comparable with ATF. Our data show that uPA-induced signal transduction takes place via uPAR, involves activation of intracellular tyrosine kinase(s) and requires an as yet undefined adaptor capable of connecting the extracellular ligand binding uPAR to intracellular transducer(s).

Keywords: GPI-anchored protein/p56/p59^{hck}/signal transduction/uPAR

Introduction

The urokinase-type plasminogen activator (uPA) and its receptor (uPAR) play an important role in a number of physiological as well as pathological extracellular degradative processes, where cell migration or tissue remodelling are required (Blasi *et al.*, 1994; Danø *et al.*, 1994). This enzymatic system acts on the cell surface by activating plasminogen to plasmin, a serine protease of broad specificity, capable of degrading fibrin and other protein components of the extracellular matrix (ECM) and of the basement membrane (Mignatti and Rifkin, 1993). In addition, uPA can influence cell migration also by directly cleaving ECM proteins, for example fibronectin (Quigley *et al.*, 1987), or by allowing activation of pro-transforming growth factor-β (pro-TGF-β) (Odekon *et al.*, 1994), and pro-hepatocyte growth factor (pro-HGF) (Naldini *et al.*, 1992, 1995) (reviewed by Fazioli and Blasi, 1994).

It has been well established that uPAR, a heavily glycosylated GPI-anchored protein with an M_r of 55 000–65 000 (Nielsen *et al.*, 1988; Ploug *et al.*, 1991), is central to many functions of uPA. In particular, activation of the single-chain pro-enzyme (pro-uPA) preferentially occurs while pro-uPA is receptor bound (Ellis *et al.*, 1989; Stephens *et al.*, 1989; Manchanda and Schwartz, 1991; Quax *et al.*, 1991); uPAR-bound uPA is fully active at the cell surface (Vassalli *et al.*, 1985) and sensitive to its specific inhibitors such as PAI-1, PAI-2 and PN-1 (Cubellis *et al.*, 1989; Ellis *et al.*, 1990). The mechanism by which inactivated uPA–PAI complexes are cleared from the cell surface via the α_2-macroglobulin receptor–low density lipoprotein receptor-related protein (Herz *et al.*, 1992; Nykjær *et al.*, 1992) is also uPAR mediated (Olson *et al.*, 1992; Conese *et al.*, 1994).

In non-migrating cells, uPAR is distributed on the cell surface at focal contacts or on the apical side, depending on the cell function (Myöhäinen *et al.*, 1993; Limongi *et al.*, 1995) while in actively migrating monocytes uPAR rapidly redistributes at the leading edge of the cells (Estreicher *et al.*, 1990). Thus, uPAR plays a pivotal role by modulating and concentrating the uPA activity at the required sites of the cell surface.

In recent years, various types of evidence have indicated the possibility of a direct intracellular signalling as an additional way by which the uPA–uPAR system can influence cell migration (Busso *et al.*, 1994; Gyetko *et al.*, 1994). Indeed, stimulation of chemotaxis or chemokinesis has been observed repeatedly following treatment with uPA derivatives devoid of enzymatic activity but with receptor binding properties, such as its N-terminal fragment (ATF) or diisopropyl fluorophosphate (DFP)-inactivated uPA (Gudewicz and Gilboa, 1987; Fibbi *et al.*, 1988; Del Rosso *et al.*, 1993; Busso *et al.*, 1994). Taken together, these findings suggest that transduction of migratory signals might be achieved as a consequence of uPAR occupancy and independently of cell surface proteolytic activity.

Very limited information is available concerning the biochemical events and intracellular transducers involved in uPAR-mediated locomotion. In pro-uPA-induced cell migration, two cytokeratins (CK-8 and CK-18) are phosphorylated specifically on serine residues by uPAR-mediated signals (Busso *et al.*, 1994). In addition, as for other GPI-anchored proteins, uPAR appears to be a

component of a macromolecular complex including four protein tyrosine kinases (PTK) of the Src family of proteins (Bohuslav *et al.*, 1995). However, no information is available as to the signal transduction role to be assigned to the association of uPAR with tyrosine kinases, in particular since uPAR lacks a transmembrane and cytoplasmic domain. The system is of particular interest as many GPI-anchored proteins have been shown to be endowed with signalling capability (reviewed by Robinson, 1991).

The high affinity of the ligand–uPAR interaction might be a potent tool to investigate the mechanism of transduction by GPI-anchored proteins. Here we show that, in the human monocytic cell line THP-1, treatment with the catalytically inactive ATF of uPA induces uPAR-dependent cell migration, uPAR clustering and time-dependent activation of p56/p59^{hck}. Moreover, we provide formal evidence for the existence of a transmembrane adaptor that allows uPAR to couple functionally with intracellular transducers.

Results

uPAR is required for stimulation of cell migration

The human uPAR (CD87), corresponding to the monocyte activation antigen Mo3 (Min *et al.*, 1992), is expressed on most circulating blood cells, particularly on monocytes (Vassalli, 1994). The human myeloid THP-1 cells, which bear many similarities to authentic mononuclear phagocytes and thus represent a good model of monocyte function (Auwerx, 1991), can bind uPA similarly to unstimulated U937 cells (Estreicher *et al.*, 1990). We tested whether THP-1 cells indeed express uPAR also by indirect immunofluorescence with purified monoclonal or polyclonal anti-uPAR antibodies. Flow cytometric analysis indicated that THP-1 cells expressed a high density of uPAR with 88.5% of cells positively stained (not shown).

Since THP-1 cells produce uPA at levels comparable with those of peripheral monocytes (Gross and Sitrin, 1990), all the experiments (unless specified) were performed after a brief treatment with an isotonic acid buffer, which is known to dissociate any endogenous receptor-bound uPA (Stoppelli *et al.*, 1986).

Migration of THP-1 cells along a uPA gradient was estimated by employing a modified Boyden chamber. As a positive control for chemotaxis, we used the formylated peptide fMet–Leu–Phe (fMLP), which is known to be a potent activator of directional migration (Goldstein, 1988). Under our experimental conditions (see Materials and methods), uPA elicited a dose-dependent chemotactic response, with a maximal effect at 10 nM ($P<0.001$, Student's *t*-test). The number of migrated cells/field was comparable with that observed in the presence of 10^{-7} M fMLP (~2.2-fold stimulation over the control) (data not shown). A similar dose-dependent effect was obtained in the presence of ATF (Figure 1), which resulted in a similar response in the 1–10 nM range ($P<0.001$). At concentrations above 10 nM, the migration began to decrease. No effect on cell migration was observed when the assay was performed in the presence of similar doses of low molecular weight (LMW) uPA (Figure 1). In order to establish that the effect was indeed due to ATF and not to an impurity, chemotaxis was performed in parallel in the presence of excess anti-ATF monoclonal antibody

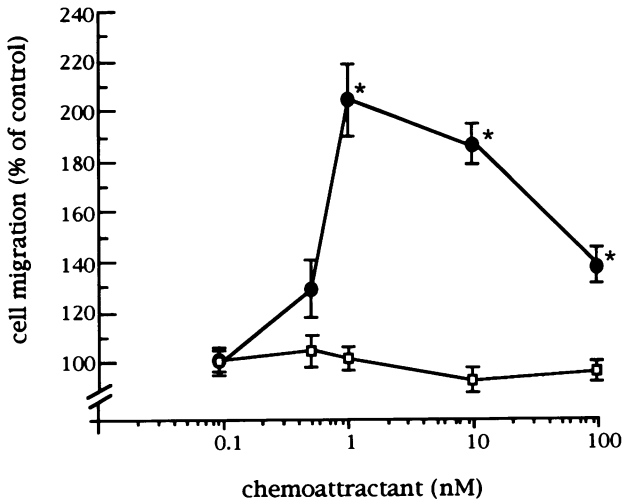

Fig. 1. Chemotactic response of THP-1 cells to ATF (–●–) and LMW uPA (–□–). Cells migrated towards a solution containing different concentrations of the indicated chemoattractant. Random cell migration was estimated as described in Materials and methods and is referred to as 100% migration. Data points represent the mean of three independent experiments (±SEM) (*$P<0.001$, Student's *t*-test).

(mAb). Under these conditions, THP-1 cells failed to respond chemotactically through the entire concentration range analysed (not shown): moreover, the antibody by itself did not influence cell migration. These findings overall confirm the data of others that uPA is a chemoattractant for THP-1 cells, and suggest that this effect only requires mere uPAR occupancy and not uPA proteolysis.

To prove that the migratory response was mediated through the specific interaction with uPAR, the effect of the anti-uPAR mAb R3, which is able to block uPA binding efficiently (Rønne *et al.*, 1991), was investigated. Therefore, before the assay, THP-1 cells were incubated either with anti-uPAR R3 mAb or with an equal amount of an isotype-matched control mAb (final concentration 10 μg/ml), washed and resuspended in serum-free medium. Results are summarized in Figure 2 (top panel): R3 pre-treated THP-1 failed to respond to the ATF gradient, indicating an impairment in transducing the chemotactic signals, while pre-treatment with control mAb showed no relevant effect on ATF-induced chemotaxis. Moreover, R3 treatment did not affect the chemotactic response to fMLP, again demostrating the uPAR specificity of the effect. To assess this result even more directly, the chemotactic property of ATF was analysed in LB6 Cl.19 cells, a murine fibroblastic cell line transfected with the human uPAR (Roldan *et al.*, 1990). The parental, untransfected, LB6 cell line, unable to bind human ATF because of the binding species specificity (Appella *et al.*, 1987; Estreicher *et al.*, 1989), was used as negative control. As shown in Figure 2 (bottom panel), ATF stimulated chemotaxis of LB6 Cl.19 cells, but not of the parental LB6 cells. On the contrary, fMLP stimulated chemotaxis in both cell lines. The concentration dependence of ATF in LB6 Cl.19 cells was similar to that in THP-1 cells (not shown).

These results clearly establish that binding of ATF to uPAR promotes a migratory signal both in THP-1 and LB6 Cl.19 cells.

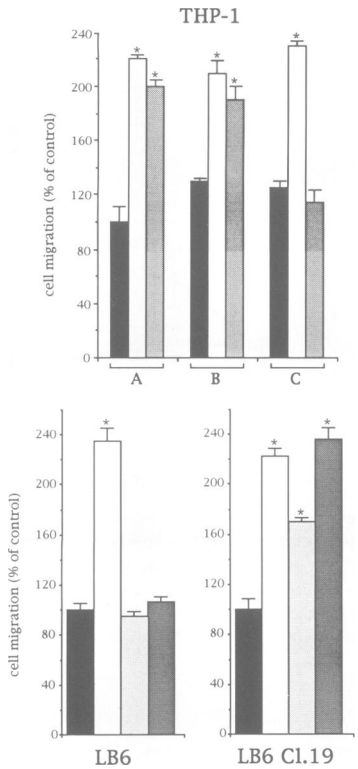

Fig. 2. Top: effect of anti-uPAR R3 mAb on THP-1 cell chemotaxis in response to ATF. Before the assay, THP-1 cells were incubated without (A) or with anti-uPAR R3 mAb [10 μg/ml (C)] or with an isotype-matched control mAb [10 μg/ml (B)] for 1 h at 4°C, washed and resuspended in medium alone. Chemotaxis was performed towards medium alone (black bars), 10^{-7} M fMLP (white bars) or 1 nM ATF (grey bars). Random cell migration of untreated THP-1 was estimated as described in Materials and methods and is referred to as 100% migration. Bottom: chemotactic response of murine LB6 and LB6 Cl.19 cells to human ATF. Cells were analysed for their ability to migrate chemotactically towards 10^{-7} M fMLP (white bars), 1 nM human ATF (light grey bars) or 10 nM human ATF (grey bars). Each point represents the mean ± SEM of three independent experiments. Random cell migration (black bars) of each cell line is referred to as 100% migration (*$P<0.001$, Student's *t*-test).

Association of uPAR with p56/p59^{hck}

In order to investigate the biochemical basis for the chemotactic function of uPAR, we first examined the pattern of phosphotyrosine-containing proteins in THP-1 cells stimulated with 1 nM ATF for different periods of time. Sequential immunoprecipitation and immunoblotting with anti-phosphotyrosine antibodies were thus performed on cell extracts. In untreated THP-1 cells, several phosphorylated species were revealed, the majority of which did not change their phosphotyrosine levels upon stimulation with ATF even after 60 min of treatment (not shown). However, despite the high background of tyrosine phosphorylation probably related to the transformed phenotype of THP-1 cells, two proteins of 75 and 38 kDa showed a significant, althought not dramatic, increase in tyrosine phosphorylation (data not shown).

These preliminary observations suggested that tyrosine phosphorylation might represent an early event following ligand binding to uPAR, and hence that uPAR might recruit and/or activate protein tyrosine kinase(s) in an early phase of signal propagation, as suggested by previous observations (Dumler *et al.*, 1993; Bohuslav *et al.*, 1995).

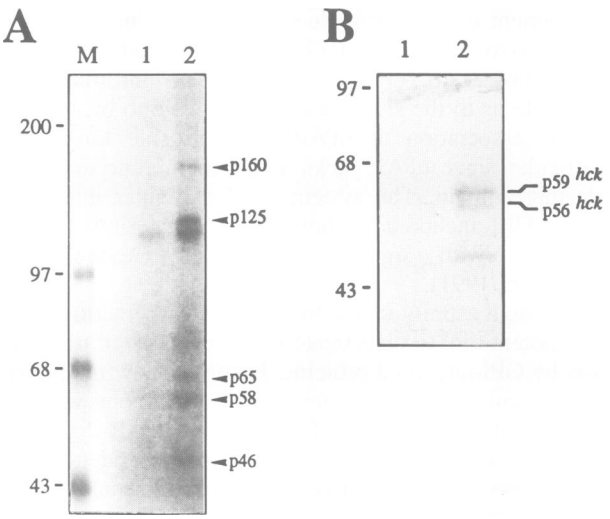

Fig. 3. Protein kinase activity in uPAR immunoprecipitates of THP-1 cells. (**A**) Kinase assays were performed using lysates from THP-1 cells immunoprecipitated using either a polyclonal anti-uPAR serum (lane 2) or the corresponding non-immune rabbit serum (lane 1). The eluates were fractionated by electrophoresis on an 8% SDS–polyacrylamide gel. Molecular mass markers ($\times 10^{-3}$) are indicated to the left. The position of phosphorylated proteins co-precipitated with uPAR is indicated by the arrowheads at the right side of the panel. Results are representative of three independent experiments. (**B**) Lysates of THP-1 cells immunoprecipitated with anti-uPAR serum were assayed for *in vitro* kinase assay as in (A). Immunocomplexes were then eluted, as indicated in Materials and methods, subjected to a second immunoprecipitation with anti-hck antibody in the presence (lane 1) or in absence of the cognate peptide (lane 2), and analysed by 10% SDS–PAGE. The positions of the two *hck* translation products (p56 and p59) are indicated by lines at the right. Molecular weight markers are shown in kDa at the left.

We therefore studied the association of uPAR with kinase activity in our cell system. THP-1 cell extracts were treated with anti-uPAR serum and the immunoprecipitates assayed for kinase activity in the presence of [γ-^{32}P]ATP. As shown in Figure 3A, lane 2, a set of phosphorylated proteins with M_rs of ~160, 125, 65, 58 and 46 kDa was present in the kinase reactions performed on immunocomplexes derived by anti-uPAR immunoprecipitation. None of these phosphorylated proteins was detected when the corresponding non-immune rabbit serum was used in the immunoprecipitation (Figure 3B, lane 1), indicating the specificity of the reaction.

GPI anchorage of uPAR was critical for uPAR-associated kinase activity. In fact, when THP-1 cells were pretreated with increasing concentrations of phosphatidylinositol-specific phospholipase C (PI-PLC) to disrupt the surface GPI anchorage, kinase activity in uPAR immunoprecipitates gradually decreased; the decrease mirrored the diminished uPAR expression, monitored by flow cytometry (not shown).

The intensity of the various bands was decreased, but not abolished by KOH treatment, suggesting that they were not phosphorylated exclusively on tyrosine residues (not shown).

We next attempted to identify the associated protein kinase(s). The favourite candidates are members of the Src family of protein tyrosine kinase (PTK), since physical association of these enzymes with uPAR has been reported recently in human monocytes (Bohuslav *et al.*, 1995). The

58 kDa phosphoprotein co-precipitated with uPAR has a molecular mass compatible with tyrosine kinases of the Src family. Among the known members of the Src family of proteins expressed on THP-1 cells, only p56/p59^{hck} co-migrated exactly with the 58 kDa protein (not shown). To prove that p58 indeed corresponded to p56/p59^{hck}, re-precipitation experiments were performed. After an *in vitro* kinase assay on uPAR immunoprecipitates (shown in Figure 3A, lane 2), proteins were eluted by treatment with lysis buffer containing 3% SDS and subsequent heating at 95°C: the eluted material was then subjected to immunoprecipitation with anti-p56/p59^{hck} peptide antibody. As shown in Figure 3B (lane 2), this second round of immunoprecipitation revealed two major species of radiolabelled proteins corresponding to p56/p59^{hck}. The specificity of the reaction was shown by the absence of the phosphorylated bands when the anti-p56/p59^{hck} antibody was pre-incubated with the cognate peptide (Figure 3B, lane 1).

Co-capping of uPAR with p56/p59^{hck}

To obtain additional evidence that p56/p59^{hck} exists in the same physical complex as the uPAR, we investigated the association of p56/p59^{hck} with uPAR *in vivo* by antibody-induced co-capping experiments.

Previous studies have shown that, in the presence of a chemotactic gradient such as fMLP, human monocytes and U937 cells polarize their uPAR at the leading edge of the cells (Estreicher *et al.*, 1990): it is thus possible that the presence of ligand influences the clustering of uPAR on the cell surface. For this reason, the ability of uPAR to form surface caps was examined on THP-1 cells before or after pre-treatment with a catalytically inactive uPA derivative (single-chain pro-uPA or ATF). We obviously tested that treatment with pro-uPA or ATF did not influence uPAR expression on the cell surface. Flow cytometric analysis indicated that uPAR levels on THP-1 cells were unchanged for at least 3 h after exposure to ligands (not shown).

Addition at 4°C of mouse anti-uPAR mAb R2 (Rønne *et al.*, 1991) to THP-1 cells, followed by fluorescein-conjugated F(ab′)$_2$ fragments of goat anti-mouse IgG, resulted in a uniform surface labelling, independently of the presence of bound pro-uPA. Warming the labelled cells to 37°C for 15 min led to the capping of uPAR. In the presence of exogenous pro-uPA, ~70 ± 12.5% of THP-1 cells showed membrane caps of uPAR (Figure 4e and i). On the contrary, capping of uPAR was less inducible in the absence of exogenously added ligand, and only 12 ± 2.8% of untreated THP-1 cells formed uPAR caps. In both cases, no capping was observed when non-specific second step F(ab′)$_2$ fragments were used to cluster the first step antibody (not shown). Similar stimulation of capping was observed when ATF was used in the test instead of pro-uPA. These results indicate that ligand binding positively influences the mobility of the receptor on the membrane, facilitating its clustering.

We next tested if antibody-induced uPAR clustering had any effect on the distribution of p56/p59^{hck} in THP-1 cells. Thus, in another series of experiments, pro-uPA-treated cells were fixed immediately after the induction of capping, permeabilized and indirectly immunolabelled with a rabbit anti-p56/p59^{hck} antibody followed by the rhodamine-conjugated F(ab′)$_2$ fragment of goat anti-rabbit IgG. In uncapped THP-1 cells, a uniform intracellular p56/p59^{hck} distribution was observed (Figure 4b). When

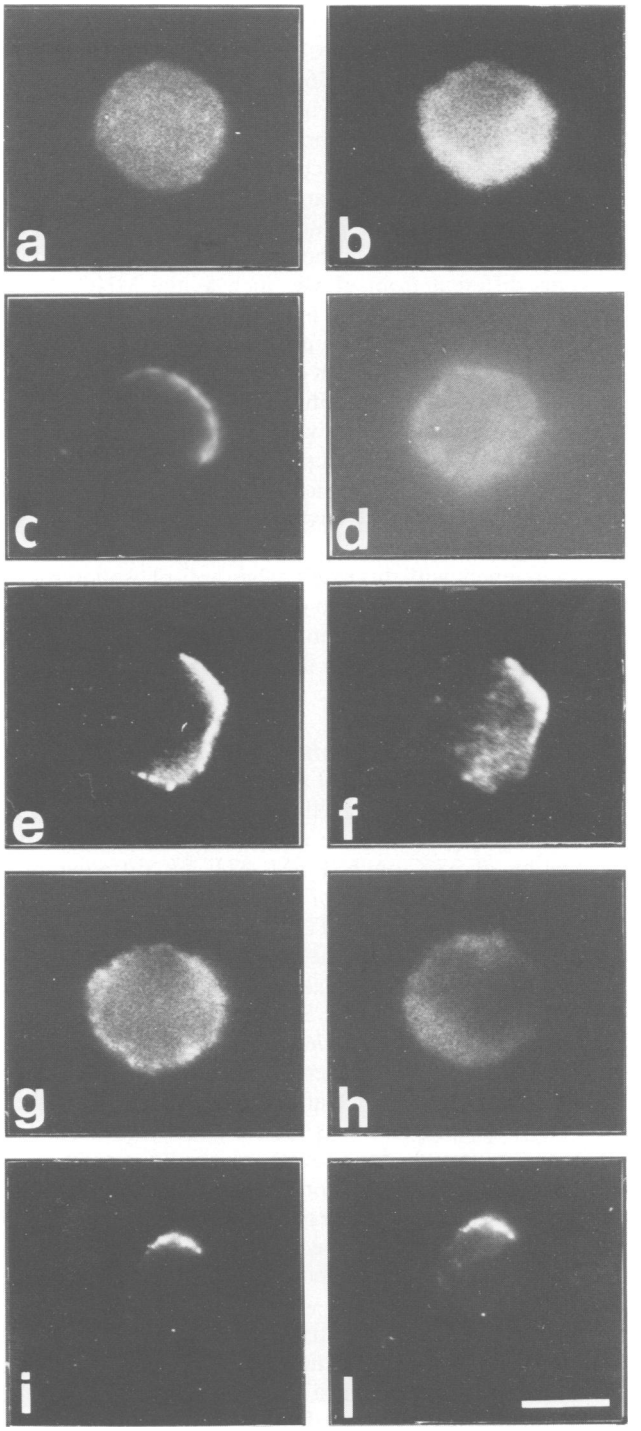

Fig. 4. Effect of uPAR capping on the intracellular distribution of p56/p59^{hck} and of phosphotyrosine-containing proteins. Cell surface uPAR or LFA-1 and intracellular p56/p59^{hck} or phosphotyrosine-containing proteins were analysed by double indirect immunofluorescent labelling in pro-uPA-treated THP-1 cells before (**a** and **g**) and after (**c, e** and **i**) antibody-induced capping. Each cell is represented by two photographs in a row. The photographs on the left illustrate the cell surface labelling of the uncapped (a and g), capped (e and i) uPAR and capped LFA-1 (c) (green channel). The photographs on the right display the intracellular p56/p59^{hck} (**b, d** and **f**) or phosphotyrosine (**h** and **l**) staining in the corresponding cell (red channel). Bar = 10 μm.

uPAR capping was promoted, p56/p59^{hck} staining co-localized with the uPAR caps (Figure 4e and f). In addition to the strong labelling of p56/p59^{hck} underneath the uPAR caps, it was always possible to observe a weak and diffuse, but still significant, membrane staining of p56/p59^{hck}, suggesting that only a fraction of the protein was co-localized with uPAR. To analyse the specificity of the association of p56/p59^{hck} with uPAR, similar experiments were performed using antibodies directed to cell surface proteins different from uPAR, such as the MHC class I antigens and the integrin leukocyte function antigen-1 (LFA-1; CD11a/CD18). Neither the capping of MHC-I antigens (not shown) nor that of LFA-1 (Figure 4c) resulted in a co-distribution of p56/p59^{hck}. In fact, a uniform intracellular p56/p59^{hck} staining was observed independently of the induction of capping (Figure 4d). We conclude from these results that physical interaction between uPAR and p56/p59^{hck} occurs *in vivo* following ligand-dependent clustering of the receptor.

In agreement with this result, when anti-phosphotyrosine antibodies were used instead of anti-p56/p59^{hck}, intracellular phosphotyrosine immunofluorescence was also found to be markedly increased in the uPAR cap regions (Figure 4g–l).

p56/p59^{hck} is activated after ligand binding

To establish a physiological role for p56/p59^{hck} in uPAR-mediated intracellular signalling, we determined the time course of p56/p59^{hck} kinase activity in THP-1 cells after incubation at 37°C with 1 nM ATF for different time periods. To ensure the use of equal amounts of p56/p59^{hck} in the *in vitro* kinase assay, THP-1 cells were metabolically labelled with [^{35}S]*Trans*Label before immunoprecipitation with anti-peptide polyclonal antibody specific for p56/p59^{hck}. Equal amounts of ^{35}S-labelled p56/p59^{hck} (Figure 5A) were analysed for *in vitro* kinase activity. As shown in Figure 5B and C, an increase in autophosphorylation of p56/p59^{hck} was observed after ATF treatment. The effect was very rapid, since it was visible already within 2 min of ligand exposure (not shown), reached a maximum in 10 min (~2.3-fold stimulation) and went back to the basal level after 30 min. The increased autokinase activity of p56/p59^{hck} was accompanied by an increase in phosphorylation of the exogenous substrate enolase (Figure 5B).

We conclude that the p56/p59^{hck} tyrosine kinase is activated following stimulation of THP-1 cells with ATF and thus may represent a downstream transducer of uPAR-mediated signal transduction. To test this point, we examined the effect of the tyrosine kinase inhibitors herbimycin A (Uehara and Fakusawa, 1991) and genistein (Akiyama and Ogawara, 1991) on ATF-induced chemotaxis. We have observed no toxic effect on THP-1 cells maintained for 96 h in the presence of 3 μM herbimycin A or 10 μM genistein (data not shown). As shown in Figure 6 (top), pre-treatment of cells with 10 μM genistein abolished the effect of ATF on p56/p59^{hck} kinase activity; similar results were obtained with herbimycin A (not shown). Importantly, herbimycin A and genistein (Figure 6, bottom) completely prevented the ATF-mediated effect on THP-1 cell migration.

The results described above indicate a specific association/activation of p56/p59^{hck} with uPAR under conditions

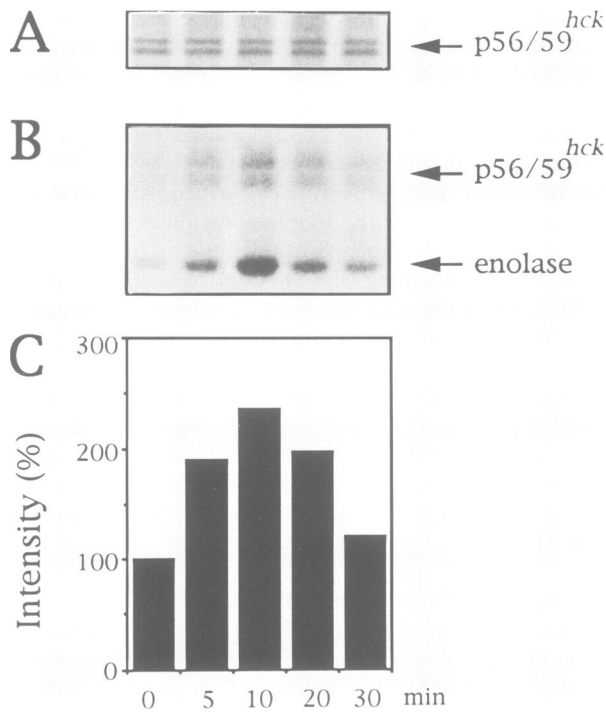

Fig. 5. Time course of p56/p59^{hck} kinase activity following ATF stimulation. THP-1 cells were metabolically labelled with [^{35}S]*Trans*Label, acid washed and either mock-treated or treated with 1 nM ATF for the indicated time at 37°C. Radiolabelled cell lysates were immunoprecipitated with an anti-p56/p59^{hck} antibody. (**A**) An aliquot from each immunoprecipitate was analysed directly by SDS–PAGE to control that equal amounts of p56/p59^{hck} were present during *in vitro* kinase assay. (**B**) The remainder of each immunoprecipitate was subjected to *in vitro* kinase assay in the presence of [γ-^{32}P]ATP and 5 μg of rabbit muscle enolase. Eluates were then analysed by SDS–PAGE and autoradiography. (**C**) The ^{32}P content of bands corresponding to p56/p59^{hck} shown in (B) was quantified by densitometric scannning of the autoradiograms and results expressed as percent of control (signal obtained from medium-treated cells). Results are representative of two independent experiments.

in which this receptor transduces the migration-promoting signal. Therefore, activation of p56/p59^{hck} can be correlated with early steps of uPAR-mediated migratory signalling.

Evidence for a transmembrane adaptor

The data presented above clearly establish that uPAR can indeed transduce a chemotactic signal. However, the question remains as to how uPAR can be coupled to the intracellular tyrosine kinase(s) in the absence of a cytoplasmic domain. A transmembrane adaptor protein might fulfil this function by contacting both extracellular uPAR and intracellular effectors. Since uPAR binding is required to promote the migratory signals, we hypothesize that a uPAR conformational change is a necessary step in the transduction process. It is known that uPA binding to uPAR or cleavage of the receptor by chymotrypsin between domain 1 (D1) and domain 2 (D2), cause a conformational change of uPAR (Behrendt *et al.*, 1991; Ploug *et al.*, 1994): this, in turn, might possibly uncover epitopes capable of recognizing a transmembrane adaptor. Thus the conformational change would convert uPAR from a receptor for uPA into a ligand for the adaptor. This hypothesis can be tested. We have cleaved with chymotryp-

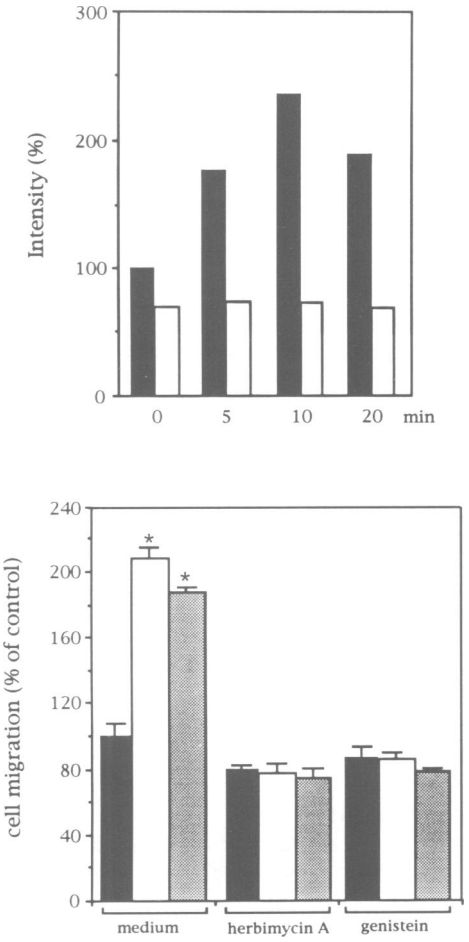

Fig. 6. Effects of tyrosine kinase inhibitors on ATF-induced signalling. Top: effect of genistein on ATF-induced increase in p56/p59^{hck} kinase activity. Cells were pre-treated for 15 min in the presence (white bars) or absence (black bars) of 10 μM genistein and then treated with 1 nM ATF for the indicated time. *In vitro* p56/p59^{hck} kinase assays were performed as described in Figure 5; autoradiograms of two independent experiments were quantitated and the results are expressed as percent of control. Bottom: effect of herbimycin A and genistein on ATF-stimulated chemotaxis. Cells were untreated or pre-treated for 12 h with 3 μM herbimycin A or for 15 min with 10 μM genistein. Cells were analysed for their ability to migrate chemotactically towards medium alone (black bars), 1 nM (white bars) or 10 nM (grey bars) human ATF. Random cell migration of untreated THP-1 cells was estimated as described in Materials and methods and is referred to as 100% migration (*P<0.001, Student's t-test).

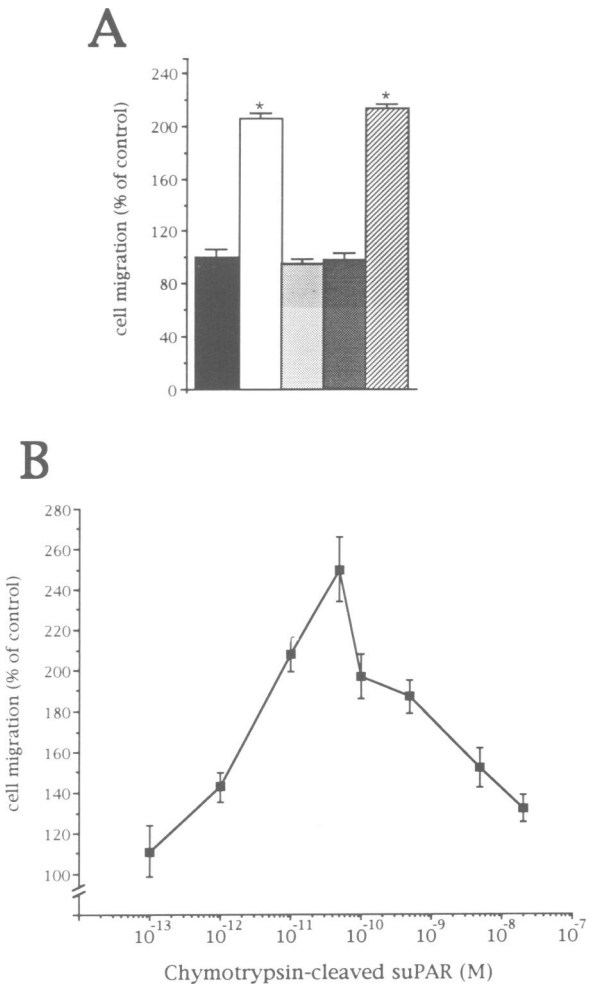

Fig. 7. (**A**) Chemotactic properties of chymotrypsin-cleaved suPAR on LB6 cell migration. LB6 murine cells migrated towards a solution containing 10^{-7} M fMLP (white bar), chymotrypsin (0.025 ng/ml) + PMSF (0.08 μM) (light grey bar), 0.5 nM suPAR (grey bar) or 0.5 nM chymotrypsin-cleaved suPAR (striped bar) Each point represents the mean ± SEM of three independent experiments. Random cell migration (black bar) is referred to as 100% migration (*P<0.001, Student's t-test). (**B**) Dose-dependent chemotactic response of LB6 cells to chymotrypsin-cleaved suPAR. Murine LB6 cells migrated towards a solution containing different concentrations of chymotrypsin-cleaved suPAR. LB6 cell migration towards medium containing chymotrypsin (1 ng/ml) and PMSF (3.2 μM) is referred to as 100% migration.

sin a purified soluble mutant of uPAR (suPAR; Masucci *et al.*, 1992) and tested it as an inducer of chemotaxis on untransfected parental murine LB6 cells. These cells should contain all the components of the uPAR signalling patways, including the hypothetical adaptor, since they can respond biologically to an ATF gradient (see Figure 2, bottom panel) when transfected with the human uPAR cDNA (i.e. LB6 Cl.19 cells). We first examined the migration of LB6 cells in the presence of a positive gradient of non-cleaved suPAR. As shown in Figure 7A, 0.5 nM suPAR did not show chemoattractant properties. Similar results were obtained when suPAR was used at concentrations up to 10 nM (not shown). On the contrary, chymotrypsin-cleaved suPAR (0.5 nM) behaved as a potent chemoattractant on LB6 cells (Figure 7A), comparable with 100 nM fMLP. Negative control experiments included the lack of effect of chymotrypsin plus phenylmethylsulphonyl fluoride (PMSF) at the same concentrations present in the suPAR-cleaved samples (Figure 7A). A dose-dependence analysis of the effect of chymotrypsin-cleaved suPAR on chemotaxis of LB6 cells is shown in Figure 7B. The effect of chymotrypsin-cleaved suPAR on LB6 cell migration was still significant at doses as low as 1 pM (Figure 7B), with half-maximal effects at 5 pM.

The ability of exogenous cleaved suPAR to stimulate chemotaxis was confirmed in LB6 Cl.19 and THP-1 cells (Table I). Concordantly, stimulation of THP-1 cells with cleaved suPAR also induced the activation of p56/p59^{hck}, with kinetics similar to those induced by ATF (Figure 8).

We consider these results as evidence for the existence of a transmembrane adaptor protein. However, the possibility exists that chymotrypsin-cleaved suPAR in fact interacts

Table I. Chemotactic effect of chymotrypsin-cleaved suPAR on THP-1 and LB6 Cl.19 cell migration

Treatment[a]	% of cells migrating (mean ± SEM)[b]	
	THP-1	LB6 Cl.19
No addition	100 ± 3.7	100 ± 6.5
fMLP 10^{-7} M	200 ± 8.7*	192 ± 10.7*
suPAR 10^{-9} M	102 ± 3.7	85 ± 12.1
Cleaved suPAR 10^{-9} M[c]	77 ± 7.2*	186 ± 5.8*
Chym. + PMSF[d]	111 ± 5.7	103 ± 3.4

[a]Cell migration was analysed as described in Materials and methods in the presence or absence of the indicated chemoattractant.
[b]The value 100% refers to the number of cells that migrated in the absence of chemoattractant. Data points are the mean ± SEM of three experiments.
[c]Chymotrypsin-cleaved suPAR was prepared as described in Materials and methods.
[d]Chymotrypsin (0.05 ng/ml) + PMSF (0.16 μM).
*$P<0.001$, Student's *t*-test.

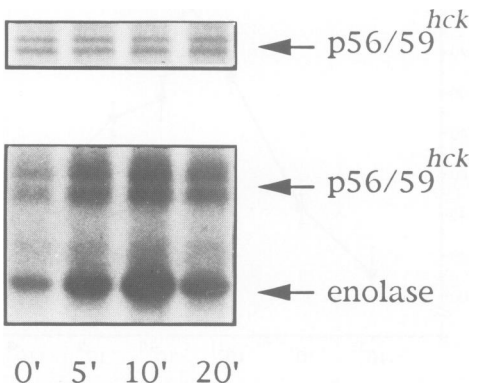

Fig. 8. Effect of chymotrypsin-cleaved suPAR on p56/p59^{hck} kinase activity in THP-1 cells. THP-1 cells were metabolically labelled with [^{35}S]*Trans*Label, acid washed and either mock-treated or treated at 37°C with 1 nM chymotrypsin-cleaved suPAR for the indicated time. Cells were then lysed, immunoprecipitated and analysed as for Figure 6.

with the membrane-bound murine uPAR present in LB6 cells. The three domains of uPAR are known to be engaged in interdomain interactions (Ploug *et al.*, 1994), and such interactions might be conserved between species. To exclude this possibility, we studied the effect of cleaved suPAR also on thioglycollate-elicited macrophages derived from uPAR$^{-/-}$ recombinant mice (Bugge *et al.*, 1995; Dewerchin *et al.*, 1996). As shown in Table II, these cells did not respond to the human ATF, or to the intact human suPAR. However, they were able to migrate efficiently towards a gradient of chymotrypsin-cleaved suPAR.

We conclude, therefore, that uPAR-induced chemotaxis most likely relies on an interaction between uPAR and an as yet uncharacterized, possibly transmembrane, adaptor.

Discussion

We show here that: (i) the chemotactic response of catalytically inactive derivatives of uPA requires binding to uPAR; (ii) binding to uPAR induces a transient activation of p56/p59^{hck}; (iii) chemotaxis can be elicited in cells lacking binding sites for human uPA by the addition of a chymotrypsin-cleaved soluble form of uPAR; and (iv)

Table II. Chemotactic effect of chymotrypsin-cleaved suPAR on thioglycollate-elicited cells obtained from uPAR$^{-/-}$ mice[a]

Treatment[b]	% of cells migrating (mean ± SEM, n = 5)[c]
No addition	100 ± 2.6
hATF 10^{-9} M	97 ± 4.1
suPAR 10^{-9} M	99 ± 5.3
Cleaved suPAR 10^{-9} M[d]	161 ± 3.9*
Cleaved suPAR 10^{-10} M[d]	186 ± 4.6*
Chym. + PMSF[e]	105 ± 6.1

[a]Adult uPAR$^{-/-}$ mice were injected with 3% thioglycollate broth into the peritoneal cavity; 4 days following injection, animals were sacrified and peritoneal cells were harvested according to Conrad (1981).
[b]Cells were allowed to migrate for 4 h at 37°C as described in Materials and methods in the presence or absence of the indicated chemoattractant.
[c]Data are expressed as mean percentage of untreated control cells ± SEM. n is the number of mice, each providing cells for one experiment.
[d]Chymotrypsin-cleaved suPAR was prepared as described in Materials and methods.
[e]Chymotrypsin (0.05 ng/ml) + PMSF (0.16 μM).
*$P<0.001$, Student's *t*-test.

chymotrypsin-cleaved suPAR also transiently induces activation of p56/p59^{hck}.

uPAR requirement

We have shown that the ATF of uPA acts as a chemoattractant in THP-1 cells as well as in murine fibroblasts expressing the human uPAR (LB6 Cl.19), inducing a dose-dependent migratory response. These results extend previous reports indicating a role for the uPA–uPAR system in the transduction of a chemotactic signal. In fact, enhanced chemotaxis and chemokinesis have been reported in different model systems, such as neutrophils (Gudewicz and Gilboa, 1987), epithelial cells (Busso *et al.*, 1994), bovine endothelium (Fibbi *et al.*, 1988) and fibroblasts (Del Rosso *et al.*, 1993). In all these studies, it has been shown that the effects did not depend on the catalytic portion of uPA, but were sustained by the ATF domain or other catalytically inactive, receptor binding forms of uPA.

In the present study, we show that uPAR is required for the induction of chemotaxis. In fact, the effect of ATF on THP-1 migration could be reproduced with two-chain uPA, but not with the LMW uPA. This latter molecule is proteolytically as active as two-chain uPA, but cannot bind uPAR (Stoppelli *et al.*, 1985). Moreover, pre-treatment of THP-1 cells with the R3 mAb, which prevents ligand binding to uPAR (Rønne *et al.*, 1991), blocked the effect of ATF. Finally, ATF was able to induce chemotaxis in murine LB6 Cl. 19 cells expressing human uPAR, but not in the parental LB6 cell line. A corollary of this result is that the parental LB6 cells must possess all signal transduction components required for chemotaxis, but do not respond to human ATF because their murine uPAR does not recognize human ATF (Appella *et al.*, 1987; Estreicher *et al.*, 1989; Olson *et al.*, 1992).

Activation of tyrosine kinase(s)

Preliminary observations suggested that uPA-delivered signals are probably propagated by intracellular phos-

phorylations (Dumler *et al.*, 1993; Busso *et al.*, 1994; Bohuslav *et al.*, 1995). Specific phosphorylation events have been reported in a human epithelial cell line in which uPAR occupancy correlated with a time-dependent increase of serine phosphorylation of cytokeratins CK18 and CK8 (Busso *et al.*, 1994). In our cell system, ATF treatment indeed induced a specific, although not dramatic, increase in the tyrosine phosphorylation contents of two proteins of 75 and 38 kDa. One of these has a molecular mass similar to the p38 protein that undergoes tyrosine phosphorylation upon uPA or diisopropyl fluorophosphate (DFP)-inactivated uPA stimulation (Dumler *et al.*, 1993; Bohuslav *et al.*, 1995).

In analogy with other GPI-anchored proteins endowed with signalling properties, uPAR appears to be associated with members of the Src family of protein tyrosine kinases (Bohuslav *et al.*, 1995), although no functional relevance of the described association has ever been provided. Taking advantage of the high sensitivity of *in vitro* kinase assay, we have shown that at least five phosphorylated proteins are co-precipitated with uPAR. One of them was identified as the member of the Src family of tyrosine kinases, p56/p59^{hck}. Association between uPAR and p56/p59^{hck} was also demonstrated *in vivo* by co-capping experiments. The presence of p56/p59^{hck} and of the other *in vitro* phosphorylated proteins in uPAR immunocomplexes isolated from unstimulated cells indicates a constitutive association.

These data are in agreement with those of Bohuslav *et al.* (1995), and with those describing similar association in various GPI-anchored receptors endowed with signalling properties (Stefanová *et al.*, 1992). However, we also have demonstrated that kinase activity of p56/p59^{hck} was stimulated following uPAR triggering with ATF. This effect was very rapid, transient and returned to the basal level within 30 min (Figure 5), strongly indicating that p56/p59^{hck} is a probable downstream effector of uPAR-mediated signal transduction. The inhibition of the ATF-induced effect by protein tyrosine kinases inhibitors (Figure 6) is in line with this possibility.

The identity of the additional phosphoproteins revealed by the kinase assay on uPAR immunoprecipitates is still unknown and is presently under investigation in our laboratory. We cannot exclude the presence of additional kinase(s) other than p56/p59^{hck} in the uPAR immunocomplexes.

Mechanism of signalling through the GPI-anchored uPAR

The main point that needs to be addressed is how uPAR can interact with p56/p59^{hck}. Based on the structure of the two proteins and their plasma membrane localization, a reasonable explanation might be the existence of an adaptor molecule connecting extracellular GPI-anchored uPAR to intracellular signal transducers, such as p56/p59^{hck}. The existence of such an adaptor is strongly suggested by the finding that a chymotrypsin-cleaved form of suPAR was a potent chemoattractant in the murine LB6 cells, as well as in THP-1 and LB6 Cl.19 cells (Figure 7 and Table I). Uncleaved suPAR, however, had no effect on cell migration, indicating that a unique conformation, uncovered by chymotrypsin cleavage, is required for the interaction with the adaptor. Chymotrypsin cleaves uPAR at residue Tyr87, producing a ligand binding domain, D1, and a D2 + D3 fragment (Behrendt *et al.*, 1991; Ploug *et al.*, 1994). This has been reproduced in our experiments (data not shown).

Altogether, these results indicate that cleavage of uPAR between D1 and D2 substitutes for the action of ATF–uPAR interaction and stimulates migratory signals. Accordingly, chymotrypsin-cleaved suPAR induced activation of p56/p59^{hck} with a time course identical to that of ATF (Figure 8). We therefore propose that ligand–receptor binding produces a conformational change that unmasks epitopes required for modulation of the adaptor-mediated transmembrane signalling; chymotrypsin cleavage of suPAR determines a similar, more stable conformational change and thus can substitute for the agonist-mediated chemotactic effect. Alternatively, ligand binding renders uPAR much more accessible to protease(s), which in turn specifically cleave(s) uPAR between domains D1 and D2; in this second hypothesis, production of uPAR fragment D2 + D3 would be a necessary step for initiating the adaptor-mediated transmembrane signalling. Our experiments do not discriminate between these two possibilities. However, the observation that a uPAR fragment containing domains D2 + D3 is present normally on the surface of different cell lines (Høyer-Hansen *et al.*, 1992; Solberg *et al.*, 1994) indicates that cleavage of uPAR between the N-terminal binding domain D1 and domain D2 also occurs *in vivo*, and therefore favours the second model.

The model requiring a proteolytic cleavage of uPAR presents analogy to that described for the thrombin receptor activation (Thien-Khai *et al.*, 1991). Inactive thrombin receptor is cleaved by thrombin, revealing a new N-terminus that in turn functions as a receptor agonist. In the case of the uPAR, it is known that it can indeed be cleaved by uPA; however, the affinity of uPA for the purified uPAR does not appear to be high enough to be physiologically significant (Høyer-Hansen *et al.*, 1992).

The functional significance of cleaved suPAR chemoattractant properties is shown by two sets of data. First, cleaved suPAR activates p56/p59^{hck} in THP-1 cells with a time course identical to that of ATF. Second, the biological cellular response is achieved at very low concentrations (Figure 7B). In conclusion, we show that chymotrypsin and, presumably, ligand binding convert uPAR into a high affinity ligand for an as yet uncharacterized cell surface adaptor, which in turn must be the real transducer of uPAR-mediated signalling.

Materials and methods

Materials

The following reagents were obtained from Lepetit SpA, courtesy of Dr M.L.Nolli: human single-chain pro-urokinase; human two-chain uPA; the catalytically active fragment of human uPA, LMW uPA; and the mouse anti-ATF mAb (5B4). ATF, the N-terminal fragment of human uPA (residues 1–143) was a kind gift of Dr J.Henkin (Abbott Laboratories, IL). The mouse anti-uPAR mAbs R2 and R3 (Rønne *et al.*, 1991) were kindly provided by Drs E.Rønne and G.Høyer-Hansen (Finsen Laboratory, Copenaghen, Denmark) and were purified by G-protein affinity cromatography (Mab-Trap Pharmacia, Uppsala, Sweden).

suPAR was purified by affinity chromatography from conditioned media of Chinese hamster ovary cells transfected with a mutant of uPAR (Masucci *et al.*, 1991). Chymotrypsin-cleaved suPAR was prepared as previously described (Behrendt *et al.*, 1991). Briefly, purified suPAR was incubated for 7 h at 37°C with α-chymotrypsin (enzyme to substrate

ratio 1:100) in 100 mM NH_4HCO_3; the reaction was stopped by addition of 1 mM PMSF. Cleavage of suPAR with production of domains D1 and D2 + D3 was controlled by SDS–PAGE and Coomassie staining and by chemical cross-linking to [^{125}I]ATF (Behrendt *et al.*, 1990). Rabbit anti-uPAR polyclonal serum was obtained by immunizing animals with purified suPAR; where specified, the anti-uPAR polyclonal serum was used after affinity purification on a suPAR-conjugated agarose column. Anti-class I mAb W6/32 was from Becton-Dickinson (Montain View, CA). The mouse mAb against the α subunit of LFA-1 was kindly provided by Dr R.E.Schmidt (Department of Immunology, Hannover School of Medicine, Germany). The rabbit polyclonal anti-phosphotyrosine serum was prepared according to Pang *et al.* (1985), and affinity-purified on agarose-coupled phosphotyramine. The affinity-purified rabbit polyclonal anti-p56/p59^{hck}(N-30) and its control peptide (corresponding to amino acids 8–37) were from Santa Cruz Biotechnology, Inc. (Santa Cruz, CA). Rhodamine-conjugated F(ab′)$_2$ fragment of goat anti-rabbit IgG, fluorescein-conjugated F(ab′)$_2$ fragment of goat anti-mouse IgG and fluorescein-conjugated F(ab′)$_2$ fragment of goat anti-rabbit IgG were from Protos Immunoresearch (San Francisco, CA). All the secondary reagents were cross-adsorbed on an appropriate rabbit or mouse IgG column to eliminate cross-species reactivities. PI-PLC from *Bacillus cereus*, rabbit muscle enolase and aprotinin were from Boehringer Mannheim GmbH. GammaBind G-Sepharose was from Phamacia (Uppsala, Sweden).

PMSF, collagen type I (C-9791) crystal violet (C-0775), fMLP (F-3506), herbimycin A (H-6647), genistein (G-6776) and mouse IgG_1, κ (MOPC-21) were from Sigma (St Louis, MO). α-Chymotrypsin from bovine pancreas was from Worthington Biochemical Corporation (Freehold, NY).

Cell culture

THP-1 cells were obtained from the American Type Culture Collection (Rockville, MD) and were grown continuously in suspension in RPMI-1640 medium (Life Technologies, Inc.) supplemented with 10% fetal calf serum (FCS). Mouse LB6 cells (Corsaro and Pearson, 1981) were grown as monolayers in Dulbecco's modified Eagle's medium (DMEM) supplemented with 5% FCS. LB6 Clone 19 cells, expressing the wild-type human uPAR (Roldan *et al.*, 1990), were cultured in the same medium, supplemented with G418 (0.4 mg/ml).

Cell treatments

Before all the experiments (unless specified), cell-bound uPA was removed from THP-1 cells by a 3 min exposure at 4°C to 50 mM glycine-HCl, 100 mM NaCl, pH 3.0. The cell suspension was then neutralized by addition of 0.2 volumes of 500 mM HEPES, 100 mM NaCl, pH 7.0.

For ATF triggering experiments *in vivo*, THP-1 cells were cultured for 48 h in serum-free RPMI supplemented with transferrin (5 μg/ml, Collaborative Research) and sodium selenite (10^{-8} M, Sigma) and then treated with ATF as described in the text.

PI-PLC treatment of THP-1 cells was performed by incubation of cells at a density of 10^6/ml in RPMI with 25 mM HEPES, pH 7.4, and different amounts of PI-PLC (range from 0.1 U/ml to 10 U/ml) for 1 h at 37°C, as previously described (Ploug *et al.*, 1991). Expression of uPAR on the cell surface following PI-PLC treatment was monitored by flow cytometry using either the anti-uPAR mAb R2 or the affinity-purified anti-uPAR serum (see below).

When appropiate, 3 μM herbimycin A or 10 μM genistein was added to the culture medium before the assays for the indicated time and maintained at the same concentrations throughout the experiments. Stock solutions of both inhibitors were prepared routinely in dimethyl sulphoxide (DMSO) and diluted, so that the final concentration of DMSO in culture medium never exceeded 0.1%.

Flow cytometric analysis

Cells were washed twice with cold medium, acid washed (see above) and then incubated for 30 min at 4°C with 20% normal human serum (NHS) in phosphate-buffered saline (PBS) to block the Fc receptor for IgG; after two washes in PBS, cells were incubated with the indicated antibodies in PBS containing 2% NHS for 1 h at 4°C. Cells were washed again with cold PBS and resuspended in PBS containing 2% NHS and fluorescein-conjugated F(ab′)$_2$ fragment of goat anti-mouse or anti-rabbit IgG. After 30 min on ice, cells were washed again and 10 000 cells were analysed using a FACScan flow cytometer (Becton Dickinson). Dead cells were excluded from the analysis based on the forward and sideways light-scattering properties. Negative controls were provided by incubation with an irrelevant isotype-matched mouse antibody (MOPC-21) or with a non-immune rabbit serum, followed by staining with the appropriate fluorescein-conjugated secondary F(ab′)$_2$ fragments.

Capping experiments

THP-1 cells were washed twice with PBS, resuspended in PBS supplemented with 2% bovine serum albumin (BSA) at 10^7/ml and incubated with 2 nM pro-uPA or ATF for 90 min at 4°C. After two additional washes with PBS, the cells were resuspended in PBS containing 10% NHS, left on ice for 15 min and incubated for 45 min with the mouse mAb R2 (10 μg/ml). Cells were washed again and then incubated with fluorescein-conjugated F(ab′)$_2$ fragments of goat anti-mouse IgG (5 μg/ml). All these steps were carried out at 4°C. After washing, the cells were either immediately plated on poly-L-lysine-coated glass coverslips and fixed (see below) to analyse uncapped cells, or shifted to 37°C for 15 min to induce capping of uPAR and then plated. The cells were fixed with 3% paraformaldehyde (w/v) in PBS, pH 7.5, at room temperature for 7 min, permeabilized with 0.2% Tween-20 in PBS and then immunolabelled with either the anti-phosphotyrosine or anti-p56/p59^{hck} affinity-purified polyclonal sera, followed by the cross-adsorbed rhodamine-conjugated F(ab′)$_2$ fragments of goat anti-rabbit IgG (5 μg/ml). The cells were washed again in PBS and the coverslips were mounted in 90% (v/v) glycerol/100 mM Tris–HCl, pH 8.5. Cells were analysed on a Zeiss Axiophot microscope equipped for epifluorescence using a ×63 oil immersion lens. Appropriate excitation and barrier filters were employed to observe the fluorescein or rhodamine fluorescence.

Chemotaxis

Chemotaxis assays were performed using modified Boyden chambers containing polyvinylpyrrolidone-free polycarbonate filters (13 mm diameter, 5 μm pore size, Nucleopore-Costar, Cambridge, MA) coated with collagen type I (100 μg/ml in PBS pH 7.4) to promote cell adhesion. The coated filters were washed with medium supplemented with 0.2% BSA and then placed in the Boyden apparatus. After acid wash, THP-1 cells were suspended at a final concentration of 10^6/ml in RPMI alone. 200 μl of the cell suspension were added above the filter in the Boyden chamber. Attractants to be tested were diluted in serum-free medium and added below the filter. The chambers were incubated in a humidified incubator at 37°C in 5% CO_2 in air for 90 min. Filters were removed, the upper surface scraped free of cells, fixed in methanol and stained with crystal violet. For each set of experiments, migration towards the assay medium served as control (random cell migration) and is referred to as 100% migration. All experiments were performed in triplicate; data are reported as number of cells counted for high power field (10 fields for each condition) and expressed as percentage of the control values.

In some experiments, THP-1 cells were acid washed, suspended in RPMI and incubated for 1 h at 4°C with the mAb R3 (10 μg/ml) or with the isotype-matched irrelevant mAb, MOPC-21 (10 μg/ml). Cells were thus washed twice with cold RPMI and chemotaxis was performed as described above.

Thioglycollate-elicited macrophages were obtained from mice by intraperitoneal injection of 3% thioglycollate broth (2 ml/mouse) followed by flushing the peritoneal cavity with PBS 4 days later. Homozygous, uPAR-deficient (uPAR$^{-/-}$) mice, generated using the vector described by Bugge *et al.* (1995), were kindly provided by Dr M.Dewerchin and P.Camerliet (V.I.B., Leuven, Belgium) (Dewerchin *et al.*, 1996).

Chemotaxis of murine LB6 and LB6 Cl.19 cells was performed following the same procedure, except that migration was allowed for 12 h, using 5×10^4 cells/sample.

Assay for protein kinase activity

THP-1 cells were washed twice in PBS and lysed on ice for 30 min with a buffer containing 10 mM Tris–HCl (pH 8.0), 1% (v/v) Nonidet P-40, 150 mM NaCl, 2 mM EDTA, 10 mM sodium orthovanadate, 20 mM sodium pyrophosphate, 50 μg/ml aprotinin and 2 mM PMSF. Lysates were clarified by centrifugation at 12 000 *g* for 20 min at 4°C. Before immunoprecipitation, the lysates were pre-cleared by incubation for 30 min at 4°C with GammaBind G-Sepharose (Pharmacia). Immunoprecipitation was performed for 2 h at 4°C with the anti-uPAR polyclonal serum and immunocomplexes were recovered by absorption to GammaBind G-Sepharose. Immunoprecipitates were then washed several times with a buffer containing 0.1% Nonidet P-40, 150 mM NaCl, 20 mM HEPES pH 8.0, and once with kinase buffer (0.1% Nonidet P-40, 6 mM $MnCl_2$, 50 mM HEPES, pH 8.0). Kinase assays were performed in 50 μl of kinase buffer containing 5–10 μCi of [γ-^{32}P]ATP (~3000 Ci/mmol, Amersham) for 5 min at room temperature. Reactions were stopped by adding SDS–PAGE sample buffer (30% glycerol,

5% SDS, 100 mM Tris–HCl, pH 7.8, β-mercaptoethanol and 0.01% bromophenol blue) and samples were heated at 95°C for 5 min. Kinase reactions were then analysed directly by SDS–PAGE and autoradiography. In some cases, gels were treated with 1 M KOH at 55°C for 2 h after electrophoresis and before autoradiography to reduce the background due to serine and threonine phosphorylation. For re-precipitation experiments, the immunocomplexes were eluted off the first set of immunoprecipitating beads by exposure to 3% SDS in 10 mM Tris–HCl, pH 7.5, 5 mM sodium orthovanadate, and heating for 15 min at 95°C. The eluted fraction was adjusted to 0.3% SDS in lysing buffer before the second round of immunoprecipitation.

For *in vitro* p56/p59^{hck} kinase assays, serum-starved THP-1 cells were metabolically labelled with [^{35}S]*Trans*Label (ICN, Costa Mesa, CA) before treatment *in vivo* with ATF. Briefly, cells were mantained in serum-free conditions for 48 h, washed twice with methionine- and cysteine-free medium and incubated overnight in the same medium in the presence of 60 μCi [^{35}S]*Trans*Label/ml. Cells were thus subjected to acid wash and treated with 1 nM ATF for the indicated time. Following radiolabelling and ATF treatment, cells were lysed with StaphA buffer (10 mM sodium phosphate, pH 7.5, 100 mM NaCl, 1% Triton X-100, 0.5% sodium deoxycholate, 0.1% SDS, 2 mM PMSF and 50 μg/ml aprotinin). Clarified extracts were normalized for the amount of incorporated ^{35}S radioactivity and immunoprecipitated with an affinity-purified anti-peptide polyclonal serum directed against amino acids 8–37 of p56/p59^{hck} or with the same serum previously incubated with the specific peptide (2 mg/ml). Half of each sample was analysed directly by SDS–PAGE; the other half was used for *in vitro* kinase assay, using the same experimental conditions described before. Immunocomplex phosphorylation of rabbit muscle enolase was assayed in the same manner, except that 5 μg of acid-denatured (Cooper *et al.*, 1984) enolase was added to each reaction mixture. The amounts of [^{32}P]p56/p59^{hck} and [^{32}P]enolase radioactivity were determined by densitometric scanning of autoradiograms obtained after shielding the low energy β-emission of ^{35}S with layers of aluminium foil. Under these conditions, we were able to determine only the high-energy β-emission of ^{32}P.

Acknowledgements

We thank Drs Jack Henkin, M.L.Nolli, E.Rønne and G.Høyer-Hansen for providing reagents. We are especially grateful to M.Dewerchin and P.Carmeliet for providing uPAR$^{-/-}$ mice. We are grateful to our colleagues Drs Paola Limongi and Massimo Conese for excellent support and stimulating discussion and to Dr Fabio Grassi for his advice in flow cytometry analysis. This work was supported by grants from Associazione Italiana Ricerca Cancro (AIRC), Consiglio Nazionale delle Ricerche (PFACRO) and Human Capital and Mobility Program of the EC (contract ERBCHRXCT 940427).

References

Akiyama,H. and Ogawara,H. (1991) *Methods Enzymol.*, **201**, 362–370.
Appella,E., Robinson,E.A., Ullrich,S.J., Stoppelli,M.P., Corti,A., Cassani,G. and Blasi,F. (1987) *J. Biol. Chem.*, **262**, 4437–4440.
Auwerx,J. (1991) *Experientia*, **47**, 22–31.
Behrendt,N. *et al.* (1990) *J. Biol. Chem.*, **265**, 6453–6460.
Behrendt,N., Ploug,M., Patthy,L., Houen,G., Blasi,F. and Danø,K. (1991) *J. Biol. Chem.*, **266**, 7842–7847.
Blasi,F. *et al.* (1994) *Fibrinolysis*, **8 Suppl. 1**, 182–188.
Bohuslav,J., Horejsí,V., Hansmann,C., Stöckl,J., Weidle,U.H., Majdic,O., Bartke,I., Knapp,W. and Stockinger,H. (1995) *J. Exp. Med.*, **181**, 1381–1390.
Bugge,T.H., Suh,T.T., Flick,M.J., Daugherty,C.C., Rømer,J., Solberg,H., Ellis,V., Danø,K. and Degen,J.L. (1995) *J. Biol. Chem.*, **270**, 16886–16894.
Busso,N., Masur,S.K., Lazega,D., Waxman,S. and Ossowski,L. (1994) *J. Cell. Biol.*, **126**, 259–270.
Conese,M., Olson,D. and Blasi,F. (1994) *J. Biol. Chem.*, **269**, 17886–17892.
Conrad,R.E. (1981) In Herscowitz,H.B., Holden,H.T., Bellanti,J.A. and Ghaffar,A. (eds), *Manual of Macrophage Methodology*, M.Dekker Inc., New York, pp. 5–11.
Cooper,J.A., Esch,F.S., Taylor,S.S. and Hunter,T. (1984) *J. Biol. Chem.*, **259**, 7835–7841.
Corsaro,C.M. and Pearson,M.L. (1981) *Somat. Cell Genet.*, **7**, 603–616.
Cubellis,M.V., Andreasen,P.A., Ragno,P., Mayer,M., Danø,K. and Blasi,F. (1989) *Proc. Natl Acad. Sci. USA*, **86**, 4828–4832.
Danø,K., Behrendt,N., Brünner,N., Ellis,V., Ploug,M. and Pyke,C. (1994) *Fibrinolysis*, **8 Suppl. 1**, 189–203.
Del Rosso,M., Anichini,E., Pedersen,N., Blasi,F., Fibbi,G., Pucci,M. and Ruggiero,M. (1993) *Biochem. Biophys. Res. Commun.*, **190**, 347–352.
Dewerchin,M., Van Nuffelen,A., Wallays,G., Bouché,A., Moons,L., Carmeliet,P., Mulligan,R. and Collen,D. (1996) *J. Clin. Invest.*, in press.
Dumler,I., Petri,T. and Schleuning,W.D. (1993) *FEBS Lett.*, **322**, 37–40.
Ellis,V., Scully,M.F. and Kakkar,V.V. (1989) *J. Biol. Chem.*, **264**, 2185–2188.
Ellis,V., Wun,T.-C., Behrendt,N., Rønne,E. and Danø,K. (1990) *J. Biol. Chem.*, **265**, 9904–9908.
Estreicher,A., Wohlwend,A., Belin,D., Schleuning,W.D. and Vassalli,J.D. (1989) *J. Biol. Chem.*, **264**, 1180–1189.
Estreicher,A., Mühlhauser,J., Carpentier,J.L., Orci,L. and Vassalli,J.D. (1990) *J. Cell Biol.*, **111**, 783–792.
Fazioli,F. and Blasi,F. (1994) *Trends Pharmacol. Sci.*, **15**, 25–29.
Fibbi,G., Ziche,M., Morbidelli,L., Magnelli,L. and Del Rosso,M. (1988) *Exp. Cell Res.*, **179**, 385–395.
Goldstein,I.M. (1988) In Gallin,J.I., Goldstein,I.M. and Snyderman,R. (eds), *Inflammation: Basic Principles and Clinical Correlates*, Raven Press, Ltd, New York, pp. 55–74.
Gross,T.J. and Sitrin,R.G. (1990) *J. Immunol.*, **144**, 1873–1879.
Gudewicz,P.W. and Gilboa,N. (1987) *Biochem. Biophys. Res. Commun.*, **147**, 1176–1181.
Gyetko,M.R., Todd,R.F.III, Wilkinson,C.C. and Sitrin,R.G. (1994) *J. Clin. Invest.*, **93**, 1380–1387.
Herz,J., Clouthier,D.E. and Hammer,R.E. (1992) *Cell*, **71**, 411–421.
Høyer-Hansen,G., Rønne,E., Solberg,H., Behrendt,N., Ploug,M., Lund,L.R., Ellis,V. and Danø,K. (1992) *J. Biol. Chem.*, **267**, 18224–18229.
Limongi,P., Resnati,M., Henandez-Marrero,L., Cremona,O., Blasi,F and Fazioli,F. (1995) *FEBS Lett.* **369**, 207–211.
Manchanda,N. and Schwartz,B.S. (1991) *J. Biol. Chem.*, **266**, 14580–14584.
Masucci,M.-T., Pedersen,N. and Blasi,F. (1991) *J. Biol. Chem.*, **266**, 8655–8658.
Mignatti,P. and Rifkin,D.B. (1993) *Physiol. Rev.*, **73**, 161–195.
Min,H.Y., Semnani,R., Mizukami,I.F., Watt,K., Todd,R.F.III and Liu,D.Y. (1992) *J. Immunol.*, **148**, 3636–3642.
Myöhänen,H., Stephens,R.W., Hedman,K., Topiovaara,H., Rønne,E., Høyer-Hansen,G., Danø, and Vaheri,A. (1993) *J. Histochem. Cytochem.*, **41**, 1291–1301.
Naldini,L. *et al.* (1992) *EMBO J.*, **11**, 4825–4833.
Naldini,L., Vigna,E., Bardelli,A., Follenzi,A., Galimi,F. and Comoglio,P.M. (1995) *J. Biol. Chem.*, **270**, 603–611.
Nielsen,L.S., Geoffrey,M.K., Behrendt,N., Picone,R., Danø,K. and Blasi,F. (1988) *J. Biol. Chem.*, **263**, 2358–2363.
Nykjær,A. *et al.* (1992) *J. Biol. Chem.*, **267**, 14543–14546.
Odekon,L.E., Blasi,F. and Rifkin,D.B. (1994). *J. Cell. Physiol.*, **158**, 396–407.
Olson,D., Pöllänen,J., Høyer-Hansen,G., Rønne,E., Sakaguchi,K., Wun,T.C., Appella,E., Danø,K. and Blasi,F. (1992) *J. Biol. Chem.*, **267**, 9129–9133.
Pang,D.T., Sharma,B.R. and Shafer,J.A. (1985) *Arch. Biochem. Biophys.*, **242**, 176–186.
Ploug,M., Rønne,E., Behrendt,N., Jansen,A.L., Blasi,F. and Danø,K. (1991) *J. Biol. Chem.*, **266**, 1926–1933.
Ploug,M., Ellis,V. and Danø,K. (1994) *Biochemistry*, **33**, 8991–8997.
Quax,P.H.A., Pedersen,N., Masucci,M.-T., Weening-Verhoeff,E.J.D., Danø,K., Verheijen,J.H. and Blasi,F. (1991) *Cell Regul.*, **2**, 793–803.
Quigley,J.P., Gold,L.I., Schwimmer,R. and Sullivan,L.M. (1987) *Proc. Natl Acad. Sci. USA*, **84**, 2776–2780.
Robinson,P.J. (1991) *Immunol. Today*, **12**, 35–41.
Roldan,A.L., Cubellis,M.V., Masucci,M.T., Behrendt,N., Lund,L.R., Danø,K. and Blasi,F. (1990) *EMBO J.*, **9**, 467–474.
Rønne,E., Behrendt,N., Ellis,V., Ploug,M., Danø,K. and Høyer-Hansen,G. (1991) *FEBS Lett.*, **288**, 233–236.
Solberg,H., Rømer,J., Brünner,N., Holm,A., Sidenius,N., Danø,K. and Høyer-Hansen,G. (1994) *Int. J. Cancer*, **58**, 877–881.
Stefanová,I., Horejsí,V., Ansotegui,I.J., Knapp,W. and Stockinger,H. (1992) *Science*, **254**, 1016–1019.
Stephens,R.W. *et al.* (1989) *J. Cell Biol.*, **108**, 1987–1995.
Stoppelli,M.P., Corti,A., Soffientini,A., Cassani,G., Blasi,F. and Assoian,R.K. (1985) *Proc. Natl Acad. Sci. USA*, **82**, 4939–4943.

Stoppelli,M.P., Tacchetti,C., Cubellis,M.V., Corti,A., Hearing,V., Cassani,G., Appella,E. and Blasi,F. (1986) *Cell*, **45**, 675–684.
Thien-Kai,H.V., Hung,D.T., Wheaton,V.I. and Coughlin,S.R. (1991) *Cell*, **64**, 1057–1068.
Uehara,Y. and Fakuzawa,H. (1991) *Methods Enzymol.*, **201**, 370–379.
Vassalli,J.D. (1994) *Fibrinolysis*, **8** Suppl. 1, 172–181.
Vassalli,J.D., Baccino,D. and Belin,D. (1985) *J. Cell Biol.*, **100**, 86–92.

Received on August 15, 1995; revised on November 9, 1995